OXFORD
SOT | Society of Toxicology
www.toxsci.oxfordjournals.org
Tox Spotlight article

TOXICOLOGICAL SCIENCES, 170(2), 2019, 549–561

doi: 10.1093/toxsci/kfz122
Advance Access Publication Date: May 27, 2019
Research Article

The TGFβ1 Receptor Antagonist GW788388 Reduces JNK Activation and Protects Against Acetaminophen Hepatotoxicity in Mice

Matthew McMillin,[*,†,‡] Stephanie Grant,[†,‡,§] Gabriel Frampton,[*,†,‡] Anca D. Petrescu,[†,‡,§] Elaina Williams,[†,‡,§] Brandi Jefferson,[†,‡] and Sharon DeMorrow[*,†,‡,§,1]

[*]Department of Internal Medicine, Dell Medical School, The University of Texas at Austin, Austin, Texas 78712; [†]Central Texas Veterans Health Care System, Austin, Texas, 78712; [‡]Department of Medical Physiology, College of Medicine, Texas A&M University Health Science Center, Temple, Texas, 76504; and [§]Division of Pharmacology and Toxicology, College of Pharmacy, University of Texas at Austin, Austin, Texas, 78712

[1]To whom correspondence should be addressed at Health Discovery Building, 1701 Trinity Street, Austin, TX 78712. Fax:(512) 495-5839. E-mail: sharon.demorrow@austin.utexas.edu.

ABSTRACT

Acute liver failure is a serious consequence of acetaminophen (APAP)-induced hepatotoxic liver injury with high rates of morbidity and mortality. Transforming growth factor beta 1 (TGFβ1) is elevated during liver injury and influences hepatocyte senescence during APAP-induced hepatotoxicity. This study investigated TGFβ1 signaling in the context of inflammation, necrotic cell death, and oxidative stress during APAP-induced liver injury. Male C57Bl/6 mice were injected with 600 mg/kg APAP to generate liver injury in the presence or absence of the TGFβ receptor 1 inhibitor, GW788388, 1 h prior to APAP administration. Acetaminophen-induced liver injury was characterized using histological and biochemical measures. Transforming growth factor beta 1 expression and signal transduction were assessed using immunohistochemistry, Western blotting and ELISA assays. Hepatic necrosis, liver injury, cell proliferation, hepatic inflammation, and oxidative stress were assessed in all mice. Acetaminophen administration significantly induced necrosis and elevated serum transaminases compared with control mice. Transforming growth factor beta 1 staining was observed in and around areas of necrosis with phosphorylation of SMAD3 observed in hepatocytes neighboring necrotic areas in APAP-treated mice. Pretreatment with GW788388 prior to APAP administration in mice reduced hepatocyte cell death and stimulated regeneration. Phosphorylation of SMAD3 was reduced in APAP mice pretreated with GW788388 and this correlated with reduced hepatic cytokine production and oxidative stress. These results support that TGFβ1 signaling plays a significant role in APAP-induced liver injury by influencing necrotic cell death, inflammation, oxidative stress, and hepatocyte regeneration. In conclusion, targeting TGFβ1 or downstream signaling may be a possible therapeutic target for the management of APAP-induced liver injury.

Key words: acute liver failure; necrosis; oxidative stress.

Acute liver failure (ALF) is a relatively uncommon hepatic disorder with high rates of morbidity and mortality. Acute liver failure in Western Europe and the United States is most commonly a result of acetaminophen (APAP) toxicity, with the prevalence in the United States approaching 50% of all cases of ALF (Bernal *et al.*, 2010, 2015). Acetaminophen can cause hepatotoxic injury that exceeds the regenerative capacity of the liver and therefore liver failure occurs. Acetaminophen-induced ALF is associated

with mitochondria dysfunction in hepatocytes, hepatic necrosis and inflammation (Blazka *et al.*, 1995; Boyd and Bereczky, 1966; Meyers *et al.*, 1988).

Acetaminophen is normally glucuronidated or sulfated and subsequently excreted in urine. However, when high concentrations are ingested, APAP is metabolized by cytochrome p450 2E1 (Cyp2E1) into the toxic metabolite *N*-acetyl-*p*-benzoquinone amine (NAPQI) (Dahlin *et al.*, 1984). Glutathione (GSH) is an antioxidant that inhibits NAPQI formation but GSH becomes depleted in the cytoplasm and mitochondria during hepatotoxic doses of APAP (Du *et al.*, 2014; Xie *et al.*, 2014). This results in the generation of oxidative stress, the phosphorylation of c-jun N-terminal kinase (JNK), mitochondrial permeability transition pore opening and ultimately cell death (Bajt *et al.*, 2006, 2007; Kon *et al.*, 2004; Nakagawa *et al.*, 2008). As multiple signaling pathways can influence JNK activity, it is possible that other proteins regulate this cell death-signaling pathway.

Transforming growth factor beta 1 (TGFβ1) is a multifunctional cytokine that plays roles in numerous cell processes including cell proliferation, growth inhibition, development, extracellular matrix formation, and cell death. Transforming growth factor beta 1 transduces its signal by binding a heterotetramer receptor complex made up of TGFβ receptor 1 (TGFβR1) and TGFβ receptor 2 ultimately resulting in the phosphorylation of SMAD2 and SMAD3 (Abdollah *et al.*, 1997; Zhang *et al.*, 1996). Transforming growth factor beta 1 has been shown to be a primary driver of hepatic fibrosis, though recently other researchers and ourselves have shown TGFβ1 is upregulated during ALF in mice, indicating it may have a direct role in acute liver injury (Bird *et al.*, 2018; McMillin *et al.*, 2014). In patients with hepatitis B that causes acute-on-chronic liver failure, there are significant increases in TGFβ1, which correlates strongly with increased disease severity and decreased survival (Yu *et al.*, 2015). In addition, hepatic TGFβ1 mRNA and plasma TGFβ1 concentrations are significantly increased in patients with APAP overdose compared with healthy controls (Miwa *et al.*, 1997). Furthermore, TGFβ1 has been shown to increase phosphorylation of JNK, which gives support that this pathway may influence signaling pathways leading to APAP-induced hepatocyte necrosis (Jablonska *et al.*, 2010).

To date, little is known about the exact role of TGFβ1 in the early stages of APAP-induced ALF. Therefore, the aims of this study were to assess the role of TGFβ1 and its downstream signaling and how they contribute to liver pathology in a mouse model of APAP hepatotoxicity. Gaining knowledge of this area may help identify the potential role of this pathway as a therapeutic target for management of APAP-induced ALF.

MATERIALS AND METHODS

Materials. GW788388 was purchased from Tocris Bioscience (Minneapolis, Minnesota). Hematoxylin QS was purchased from Vector Laboratories (Burlingame, California). Catalyst alanine aminotransferase (ALT) and aspartate aminotransferase (AST) assays were purchased from IDEXX Laboratories (Westbrook, Maine). Antibodies against TGFβ1, proliferating cell nuclear antigen (PCNA), phosphorylated JNK (pJNK), and JNK were purchased from Santa Cruz Biotechnology (Dallas, Texas). Interleukin 1 beta (IL-1β) and tumor necrosis factor alpha (TNFα) Duoset ELISA kits were purchased from R&D Systems (Minneapolis, Minnesota). A TGFβ1 ELISA kit and superoxide dismutase 1 (SOD1) antibody were purchased from Invitrogen (Carlsbad, California). The GSH assay, terminal deoxynucleotidyl transferase dUTP nick end labeling (TUNEL) staining kit and Cyp2E1 antibody were purchased from Abcam (Cambridge, Massachusetts). PathScan Phospho-Smad3 (pSMAD3) (Ser423/425) Sandwich ELISA Kit and a pSMAD3 antibody were purchased from Cell Signaling Technology (Danvers, Massachusetts). All other chemicals and reagents were purchased from MilliporeSigma (Burlington, Massachusetts) unless otherwise noted, and were of the highest grade available.

APAP model of ALF. *In vivo* experiments were performed using fasted male C57Bl/6J (25–30 g; The Jackson Laboratory, Bar Harbor, Maine). Acute liver failure was induced in mice via a single intraperitoneal injection of 600 mg/kg of APAP dissolved in warm saline. In a subgroup of mice, the TGFβR1 antagonist, GW788388, was injected into the peritoneum at 1 mg/kg 1 h prior to APAP injection. After APAP injection, mice were placed on heating pads set to 37°C to ensure they remained normothermic. Hydrogel and rodent chow were placed on cage floors to ensure access to food and hydration. At multiple time points up to 24 h following APAP injection, mice were euthanized and tissue and serum were collected. For mice pretreated with GW788388 or DMSO, mice were euthanized 2, 4, or 6 h following APAP or saline injection. All animal experiments in this study were performed in accordance with the Animal Welfare Act, and the Guide for the care and use of Laboratory Animals, and were approved by the Baylor Scott & White Health IACUC committee.

Primary hepatocyte culture and treatment. All perfusion solutions were prepared freshly and warmed to 37°C before use.

Mice were anesthetized with isoflurane and perfused through the right atrium of the heart into the inferior vena cava, with a solution of HBSS (Hank's balanced salt solution) supplemented with 10 mM HEPES, 0.5 mM EGTA, and 0.5 mg/ml gentamicin sulfate. The perfused solution drained via the portal vein which was cut before starting the perfusion. After this perfusion, the liver was placed into a sterile Kimax dish, and further perfused with 1–2 mg/ml collagenase B (Roche Diagnostics, Indianapolis, Indiana) in HBSS supplemented with 5 mM $CaCl_2$, for 15 min. The remaining cell slurry was passed through 100 μm cell strainers to remove any undigested liver tissue. The cells were washed with ice cold DMEM/F12 medium containing HEPES (10 mM) and FBS (10%). After centrifugation at 50 × g for 5 min, the cells were mixed with 30% Percoll (GE Healthcare Life Sciences, Pittsburgh, Pennsylvania), in DMEM/F12/HEPES/FBS medium, and spun at 200 × g for 7 min. The pelleted cells were washed with medium to remove all Percoll. The cells were counted and seeded at a density of 0.25×10^6 cells/well in 6-well plates coated with a solution of rat collagen type I. Over 95% of cells had hepatocyte characteristics, being binucleated, polygonal cells. The hepatocytes were incubated in DMEM/F12/HEPES/FBS medium for the next 24 h, and then maintained in William's E medium containing cell maintenance supplements (Combo kit CM400 from Gibco), at 37°C, 5% CO_2. The maintenance medium was changed every 2 days, and the cells were treated with 10 μM–10 mM APAP for 24 h 3–4 days after being plated.

Liver histology and function assessments. Paraffin-embedded livers were cut into 4 μm sections and mounted onto positively charged slides (VWR, Radnor, Pennsylvania). Slides were deparaffinized and stained with Hematoxylin QS (Vector Laboratories) followed by staining with eosin Y (Amresco, Solon, Ohio) and rinsed in 95% ethanol. The slides were then dipped into 100% ethanol and subsequently through 2 xylene

washes. Coverslips were mounted onto the slides using CytoSeal XYL mounting media (ThermoFisher). The slides were viewed and imaged using an Olympus BX40 microscope with an Olympus DP25 imaging system (Olympus, Center Valley, Pennsylvania). Necrotic areas were calculated using ×20 field views, drawing areas devoid of hepatocyte nuclei and area was calculated using ImageJ software (National Institutes of Health, Bethesda, Maryland). In each mouse, the necrosis from 10 fields was quantified and averaged together to determine necrotic area.

Liver function was assessed by measuring serum ALT and AST levels using a Catalyst One serum chemistry analyzer from IDEXX Laboratories, Inc. In addition, hepatic GSH levels were measured in liver homogenates using a commercially available kit according to instructions from the manufacturer. Levels of GSH were normalized to total protein of lysate.

TUNEL assay and immunohistochemistry. TUNEL assays and immunohistochemistry were performed on liver sections cut and deparaffinized as outlined above. The TUNEL assay was performed according to the protocol supplied from the manufacturer with no modifications. For immunohistochemistry, antibodies against TGFβ1, pSMAD3, and PCNA were incubated overnight at 4°C. Subsequent secondary antibody incubation and color development using 3,3′-diaminobenzidine substrate was performed using kits from Vector Laboratories according to the manufacturer's instructions. Sections were counterstained with Hematoxylin QS. TUNEL and immunohistochemical stained slides were scanned by a Leica SCN400 digital slide scanner. Transferase dUTP nick end labeling and pSMAD3 staining was quantified by converting images to grayscale and quantifying positive staining area using ImageJ software. Proliferating cell nuclear antigen quantifications were calculated by manually counting ten ×20 fields per mouse for positively stained hepatocytes.

ELISA assays. Livers were homogenized using a Miltenyi Biotec gentleMACS Dissociator (San Diego, California) and total protein was quantified using a ThermoFisher Pierce BCA Protein Assay kit (Waltham, Massachusetts). For the Mouse Duoset IL-1β and TNFα ELISA kits, capture antibodies were incubated overnight in 96-well plates. After this, the assay was performed according to the instructions provided from R&D Systems. PathScan Phospho-Smad3 (Ser423/425) Sandwich ELISA kit was performed in liver lysates according to the instructions from Cell Signaling Technology. The ThermoFisher TGFβ1 ELISA kit was performed in liver lysates, serum, or primary hepatocyte supernatants according to manufacturer's instructions, except the acid activation step was skipped to ensure that only activated TGFβ1 was measured in our samples. For each ELISA kit, the total input for each sample was 100 μg of protein or 100 μl of undiluted conditioned cell media. Absorbance was read using a SpectraMax M5 plate reader from Molecular Devices (Sunnyvale, California). Data were reported as TGFβ1, pSMAD3, IL-1β, or TNFα concentration per mg of total lysate protein or per ml of conditioned cell media.

Immunoblotting. Liver tissue was homogenized using a Miltenyi Biotec gentleMACS Dissociator and total protein was quantified using a ThermoFisher Pierce BCA Protein Assay kit. SDS-PAGE gels (10%–15% v/v) were loaded with 20–40 μg of protein diluted in Laemmli buffer per each tissue sample. Specific antibodies against Cyp2E1, pJNK, JNK, SOD1, and β-actin were used. All imaging was performed on an Odyssey 9120 Infrared Imaging System (LI-COR, Lincoln, Nebraska). Data are expressed as fold change in fluorescent band intensity of target antibody divided by β-actin or JNK, which were used as loading controls. The values of vehicle or control groups were used as a baseline and set to a relative protein expression value of 1. Band intensity quantifications were performed using ImageJ software.

Statistical analyses. All statistical analyses were performed using Graphpad Prism software (Graphpad Software, La Jolla, California). Results were expressed as mean ± SEM. For data that passed normality tests, significance was established using the Student's *t* test when differences between 2 groups were analyzed, and analysis of variance when differences between 3 or more groups were compared followed by a post hoc Tukey test. If tests for normality failed, 2 groups were compared with a Mann-Whitney U test or a Kruskal-Wallis ranked analysis when more than 2 groups were analyzed. Differences were considered significant for p values less than .05.

RESULTS

APAP Administration Generated Hepatocyte Necrosis and Depleted GSH

Acetaminophen injection into mice was initially validated to cause significant hepatotoxic liver injury with centrilobular necrosis becoming evident 2 h following APAP injection and progressing throughout the 24 h time course (Figs. 1A and 1B). This increase in necrosis was mirrored by significantly elevated concentrations of serum ALT (Figure 1C) and serum AST (Figure 1D) in APAP-treated mice beginning 2 h after injection when compared with vehicle-treated mice. As APAP-hepatotoxicity is dependent on a depletion of hepatic GSH, we assessed GSH levels which were significantly suppressed in our APAP-treated mice until 6 h following injection when compared with vehicle-treated mice (Figure 1E).

TGFβ1 Signaling Was Upregulated During APAP-Induced Hepatotoxicity

By immunohistochemical staining, TGFβ1 expression was increased in APAP-treated mice compared with saline-treated controls with staining concentrated around areas of hepatic necrosis with expression observed in hepatocytes outside the necrotic area in the 2 and 4 h post acetaminophen-treated groups (Figure 2A). Transforming growth factor beta 1 protein expression was significantly increased in liver homogenates from APAP-treated mice at 2, 4, and 6 h following APAP administration when compared with control mice (Figure 2B). This increase in hepatic TGFβ1 expression was also found in the serum, with significantly increased expression found in all APAP-treated mice 2 h following injection with the highest concentrations observed 4 and 6 h following acetaminophen administration (Figure 2C). To see if hepatocytes were able to increase their expression of TGFβ1 during APAP-induced liver injury, TGFβ1 was measured in the media of primary hepatocytes treated with increasing concentrations of APAP. The treatment of primary hepatocytes with APAP at 100 μM, 1 mM, or 10 mM concentrations led to a significant increase in secreted TGFβ1 compared with the basal group (Figure 2D).

To determine if TGFβ1 signaling was being transduced, phosphorylation of SMAD3 was measured and was found to be increased in the livers from APAP-treated mice compared with control-treated mice, with staining found predominately in

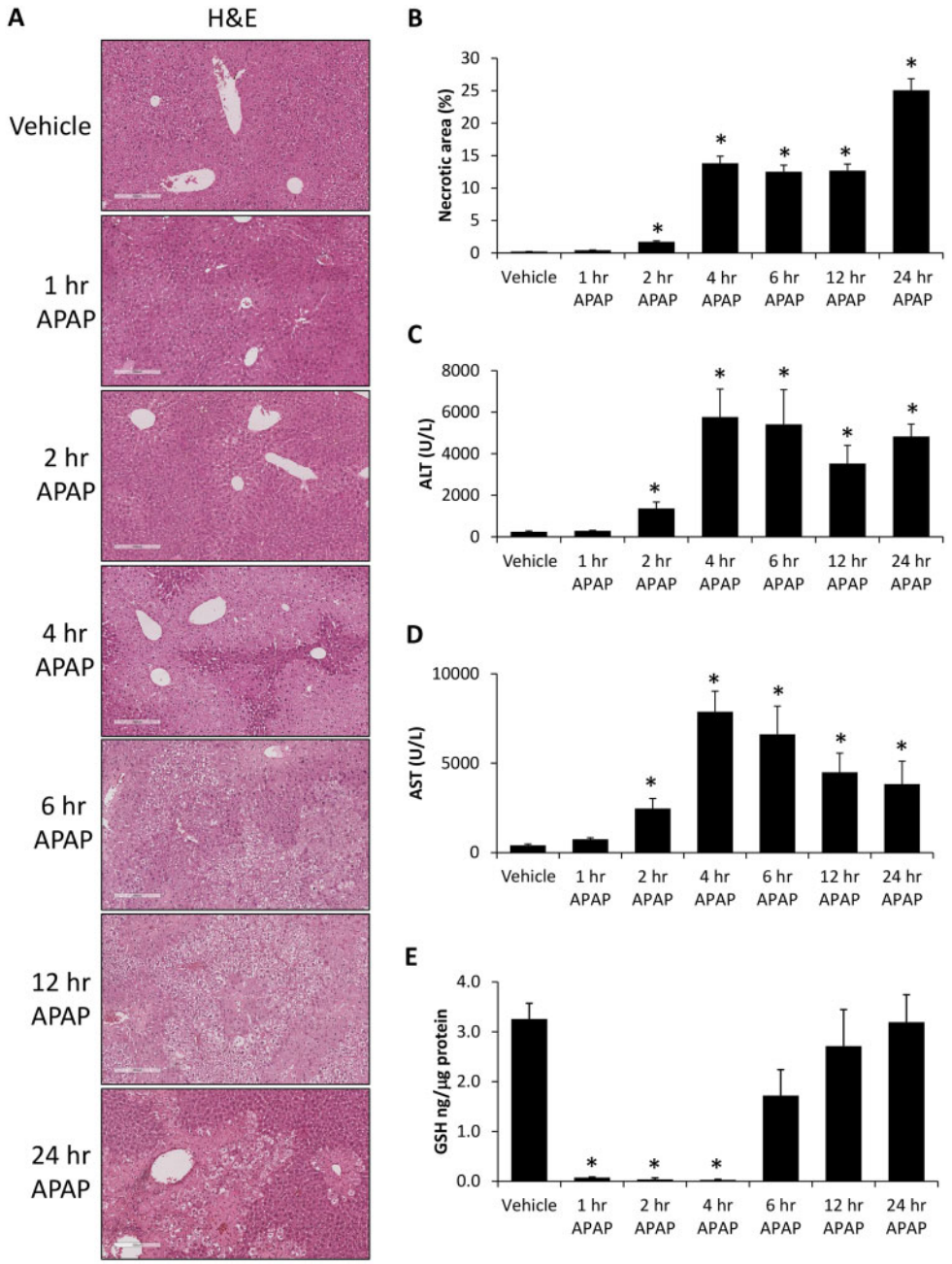

Figure 1. Acetaminophen-induced liver injury and hepatic necrosis. A, Hematoxylin and eosin (H&E) stains in liver sections from vehicle and time course APAP-treated mice. B, Percentage of hepatic necrosis calculated from H&E images in vehicle and time course APAP-treated mice. C, Serum ALT concentration in vehicle and time course APAP-treated mice. D, Serum AST concentration in vehicle and time course APAP-treated mice. E, Hepatic GSH levels measured in vehicle and time course APAP-treated mice. *$p < .05$ compared with vehicle-treated mice.

hepatocytes neighboring necrotic tissue (Figure 3A). There was a significant increase in pSMAD3 expression at 4 h following APAP administration that remained significantly elevated up to 24 h after injection (Figure 3B).

GW788388 Treatment Reduced APAP-Induced Liver Injury

In an effort to determine if the elevation of TGFβ1 in livers from APAP-treated mice contributed to pathology, TGFβ1 signaling was inhibited *in vivo* through injection of the TGFβR1 antagonist GW788388 into vehicle- and APAP-treated mice. GW788388 treatment significantly reduced centrilobular necrosis in APAP-treated mice 6 h following APAP injection compared with DMSO-treated controls (Figs. 4A and 4B). In addition, ALT and AST were significantly reduced in GW788388-treated APAP mice 6 h after APAP injection compared with DMSO-treated APAP mice (Figs. 4C and 4D). Hepatic GSH levels were significantly suppressed in both DMSO- and GW788388-treated APAP mice with GW788388 treatment leading to a significant decrease in vehicle-treated mice but no significant differences in the APAP-treated groups at any measured time point (Figure 4E). The only significant changes observed regarding necrosis, ALT and AST occurred 6 h following APAP injection, therefore the remainder of this study focused on this time point after APAP injection.

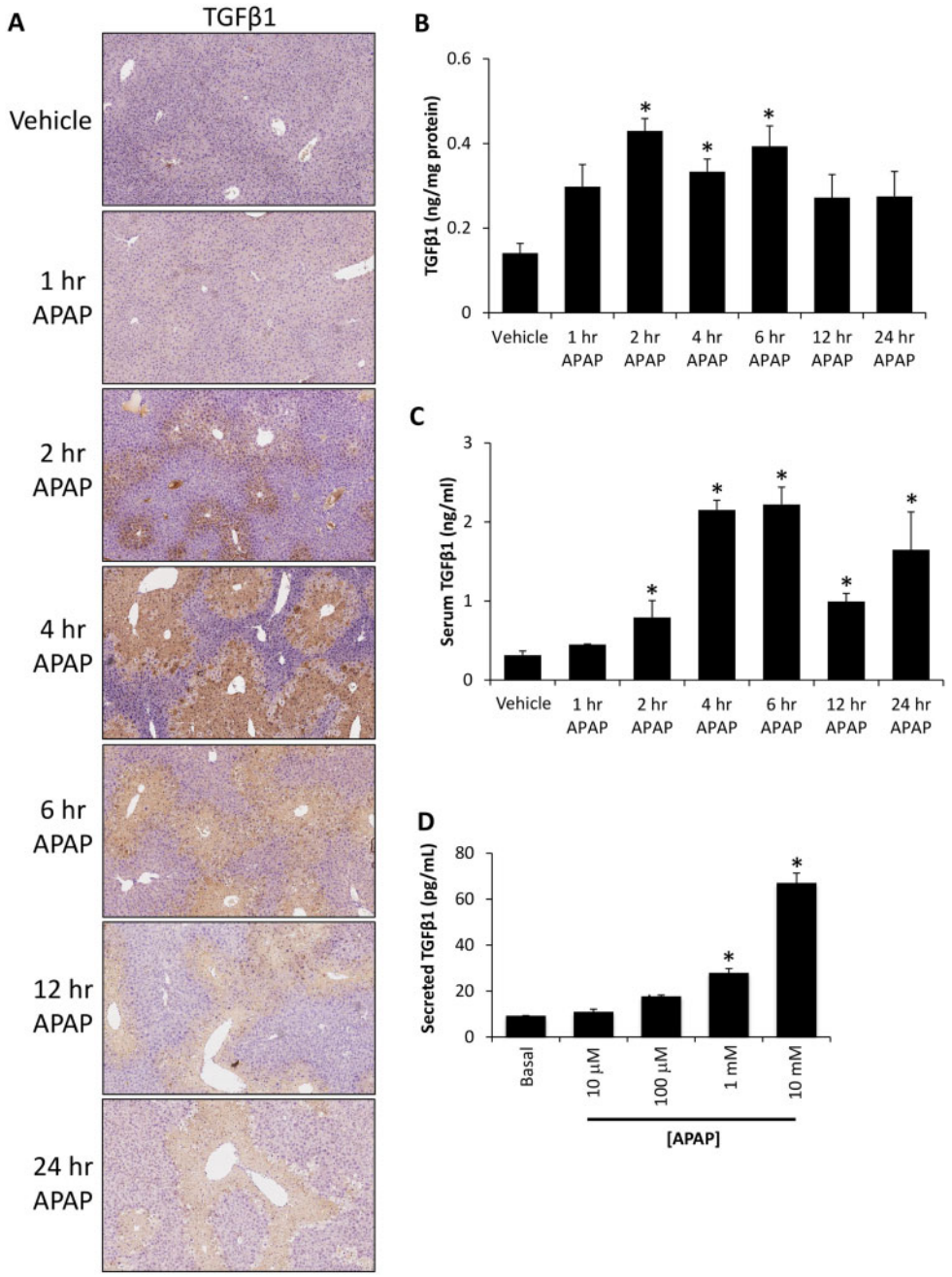

Figure 2. Hepatic TGFβ1 signaling was increased in APAP-treated mice. A, Images of immunohistochemistry for TGFβ1 in liver sections from vehicle and time course APAP-treated mice. B, TGFβ1 concentration in liver homogenates from vehicle and APAP-treated time course mice as measured with ELISA. C, Serum TGFβ1 levels as measured by ELISA in samples from vehicle and time course APAP-treated mice. D, TGFβ1 concentration measured by ELISA in conditioned media from primary hepatocytes treated with the indicated doses of APAP. *$p < .05$ compared with vehicle-treated mice.

To see if the hepatoprotective effects of GW788388 could be a result of changes in APAP metabolism, hepatic Cyp2E1 expression was assessed. Cyp2E1 expression was found to be significantly decreased in DMSO-treated APAP mice and not in GW788388-treated mice (Figs. 5A and 5B).

Hepatic Cell Death, Inflammation, and Oxidative Stress Were Reduced in APAP-Treated Mice Administered GW788388

Because GW788388 treatment reduced APAP-induced liver injury, its direct inhibition of TGFβ1 signaling and its downstream consequences were assessed. By immunohistochemistry, GW788388 treatment attenuated the APAP-induced increase in pSMAD3 immunoreactivity (Figure 6A). These findings were validated with ELISA assays, which demonstrated a significant increase in pSMAD3 levels in APAP + DMSO-treated mice when compared with DMSO-treated controls or the GW788388-treated mice groups (Figure 6B). Furthermore, because TGFβ1 signaling has been demonstrated to increase JNK phosphorylation thereby promoting hepatocyte cell death during APAP-induced liver injury (Xie *et al.*, 2014), pJNK expression was assessed in GW788388-treated mice. There was increased phosphorylation of JNK in liver homogenates from APAP + DMSO-treated mice compared with the vehicle-treated groups and treatment with GW788388 significantly reduced pJNK expression in APAP-

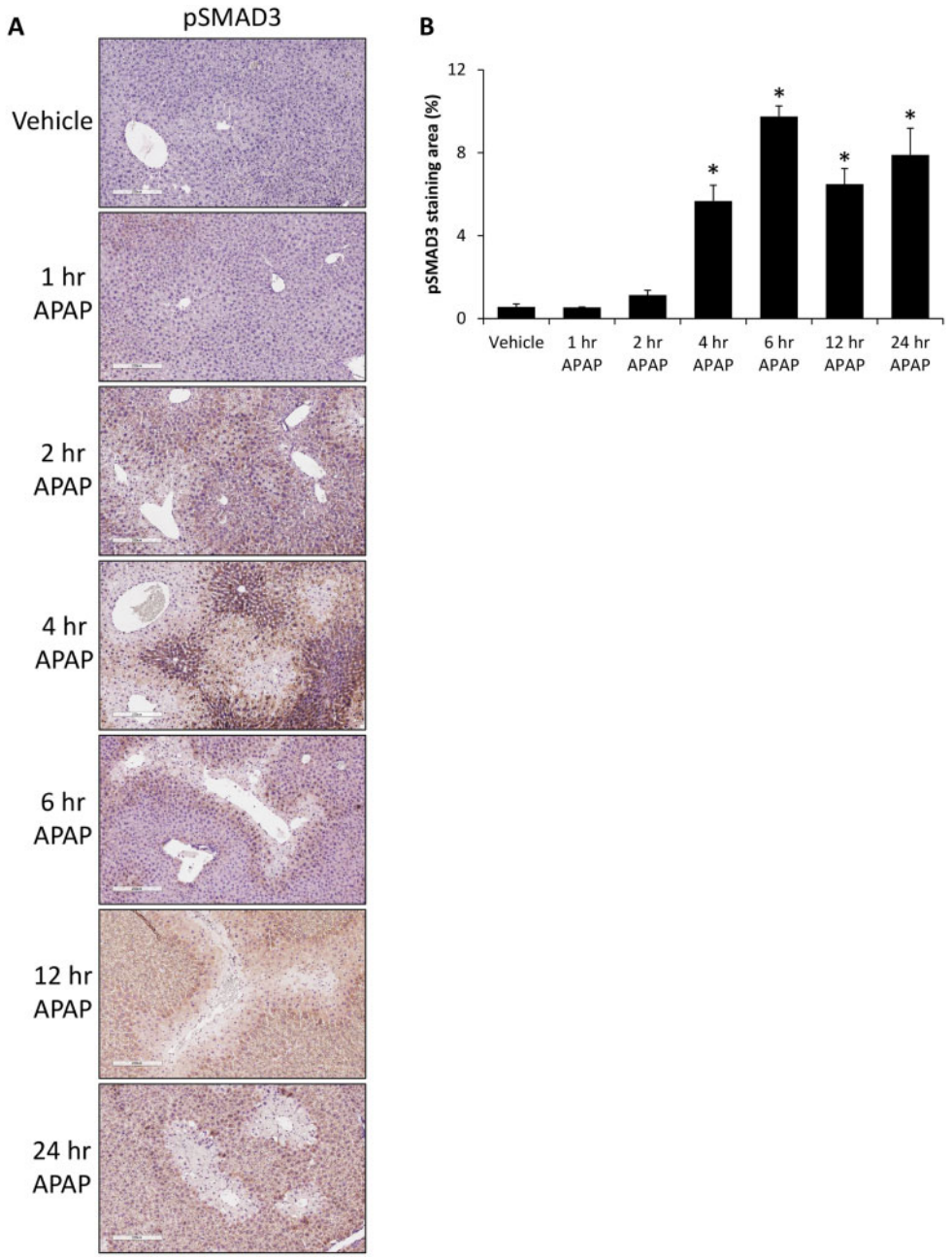

Figure 3. Phosphorylation of SMAD3 in increased in APAP-treated mice. A, Images of immunohistochemistry for pSMAD3 in liver sections from vehicle and time course APAP-treated mice. B, Quantification of pSMAD3 expression in immunohistochemical images in vehicle and time course APAP-treated livers. *$p < .05$ compared with vehicle-treated mice.

treated mice (Figs. 6C and 6D). As JNK signaling can lead to necrotic cell death, DNA fragmentation was assessed by TUNEL staining. There was a significant increase in hepatic TUNEL staining in APAP and DMSO-treated mice that was significantly reduced in APAP and GW788388-treated mice (Figs. 6E and 6F).

As an early event following APAP-induced liver injury, there is increased production of pro-inflammatory cytokines, recruitment of immune cells, and increased oxidative stress in the liver (Du *et al.*, 2016). In this study, hepatic expression of IL-1β and TNFα were significantly increased in APAP + DMSO-treated mice compared with vehicle-treated mice and APAP + GW788388-treated mice had significantly reduced levels compared with APAP + DMSO-treated mice (Figs. 7A and 7B). The expression of SOD1, a protein that reduces oxidative stress by catalyzing the formation of oxygen and hydrogen peroxide from superoxide (McCord and Fridovich, 1969), was decreased in APAP-treated mice administered DMSO compared with mice treated with APAP + GW788388, which demonstrates that TGFβ1 signaling inhibits the ability of the liver to handle oxidative stress (Figs. 7C and 7D).

Pretreatment With GW788388 Promotes Proliferation of Hepatocytes Following APAP-Induced Injury

As APAP-induced hepatic injury is known to stimulate hepatocyte proliferation as a mechanism to restore liver function, PCNA immunostaining and quantification were performed. APAP-treated mice had significantly increased staining for PCNA compared with

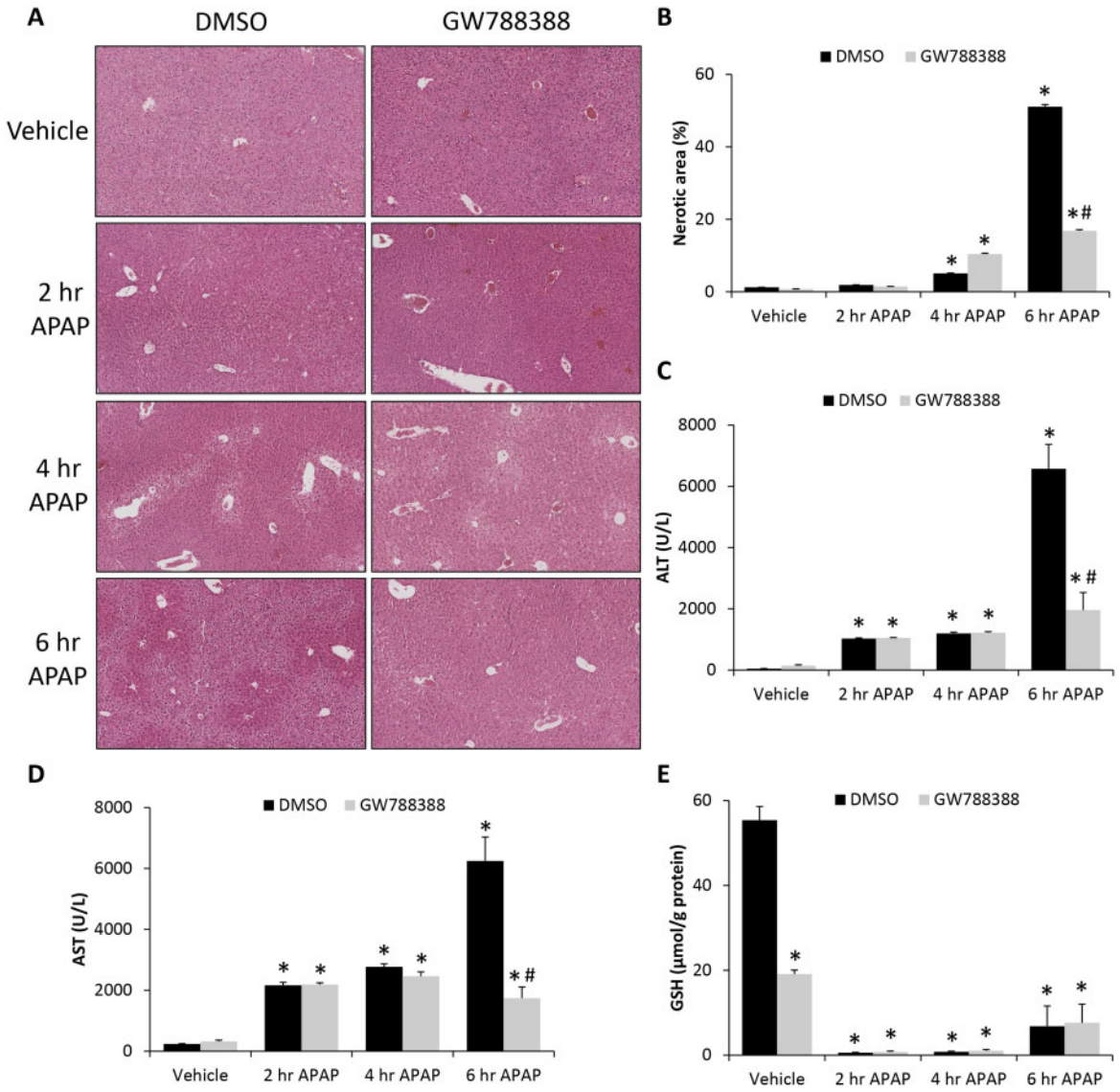

Figure 4. GW788388 treatment reduced APAP-induced liver injury. A, Hematoxylin and eosin (H&E) stains in liver sections from vehicle and time course APAP-treated mice injected with DMSO or GW788388. B, Percentage of hepatic necrosis calculated from H&E images in vehicle and time course APAP-treated mice injected with DMSO or GW788388. C, Serum ALT concentration in vehicle and time course APAP-treated mice injected with DMSO or GW788388. D, Serum AST concentration in vehicle and time course APAP-treated mice injected with DMSO or GW788388. E, Hepatic GSH levels measured in vehicle and time course APAP-treated mice injected with DMSO or GW788388. *$p < .05$ compared with vehicle-treated mice injected with DMSO. #$p < .05$ compared with DMSO-treated mice injected with APAP at same time point.

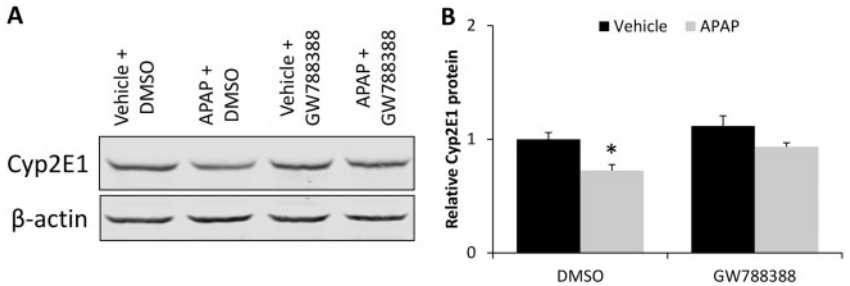

Figure 5. Inhibition of TGFβ1 signaling restored decreased Cyp2E1 expression in APAP-treated mice. A, Immunoblot for Cyp2E1 in liver homogenates from vehicle and APAP-treated mice injected with DMSO or GW788388 with β-actin used as a loading control. B, Quantification of Cyp2E1 and β-actin immunoblots in livers from vehicle and APAP-treated mice injected with DMSO or GW788388. *$p < .05$ compared with vehicle-treated mice injected with DMSO.

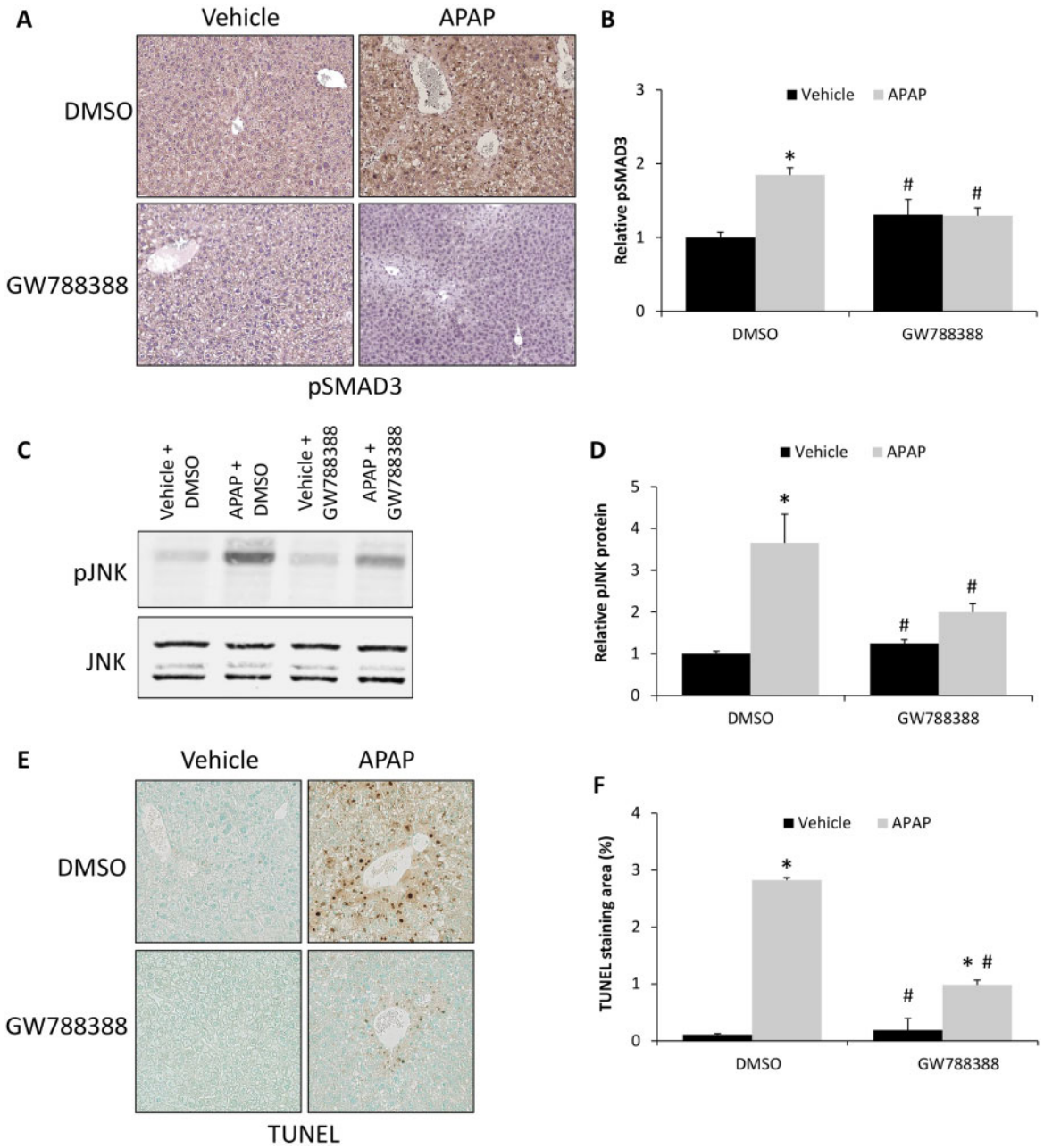

Figure 6. TGFβ1-induced hepatocyte cell death was reduced in APAP-treated mice by treatment with GW788388. A, Immunohistochemistry for pSMAD3 in liver sections from vehicle and 6 h APAP-treated mice injected with DMSO or GW788388. B, Relative pSMAD3 protein expression as measured by ELISA assay in vehicle and 6 h APAP-treated mice administered DMSO or GW788388. C, Immunoblot for pJNK and JNK in liver homogenates from vehicle and 6 h APAP-treated mice injected with DMSO or GW788388. D, Quantification of pJNK and JNK immunoblots in livers from vehicle and 6 h APAP-treated mice injected with DMSO or GW788388. E, TUNEL staining images in liver sections from vehicle and 6 h APAP-treated mice injected with DMSO or GW788388. F, Quantification of TUNEL staining in vehicle and 6 h APAP-treated mice injected with DMSO or GW788388 expressed in percent area. *$p < .05$ compared with vehicle-treated mice injected with DMSO. #$p < .05$ compared with 6 h APAP-treated mice injected with DMSO.

vehicle-treated controls (Figs. 8A and 8B). Most cells staining positive for PCNA were hepatocytes and mice pretreated with GW788388 had an even greater number of PCNA-stained hepatocytes compared with DMSO-treated controls (Figs. 8A and 8B).

DISCUSSION

The data presented support that APAP-induced hepatic injury led to increased TGFβ1 expression and downstream signaling in the liver and increased TGFβ1 levels in the serum. TGFβ1 ligand expression was found predominately in areas of hepatic necrosis whereas phosphorylation of SMAD3 was observed in hepatocytes in perinecrotic areas. Inhibition of TGFβ1 signaling via GW788388 treatment reduced hepatic necrosis, liver injury, and improved liver function through the reduction of hepatocyte cell death and hepatic inflammation. A working schematic of TGFβ1 signaling in the context of APAP-induced hepatotoxicity is presented in Figure 9. Together, the data

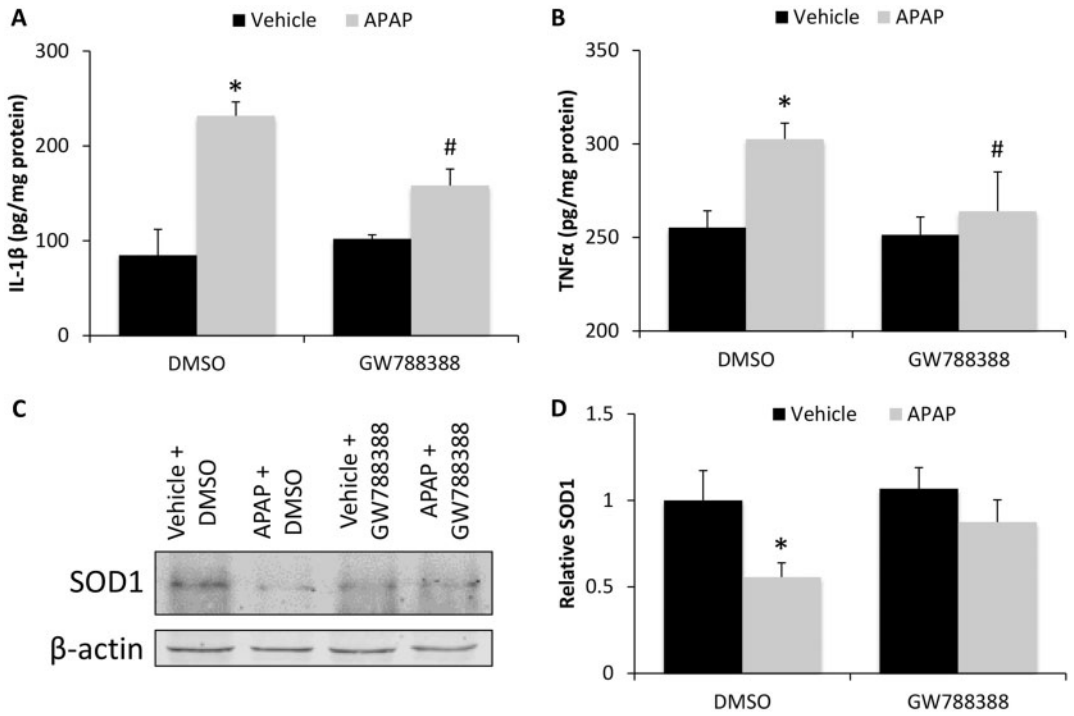

Figure 7. Hepatic inflammation and oxidative stress in APAP-treated mice was increased by TGFβ1 signaling. A, IL-1β protein concentration as measured by ELISA assay in liver homogenates from vehicle and 6 h APAP-treated mice injected with DMSO or GW788388. B, TNFα protein concentration as measured by ELISA assay in liver homogenates from vehicle and 6 h APAP-treated mice injected with DMSO or GW788388. C, SOD1 immunoblot in liver homogenates in vehicle and 6 h APAP-treated mice administered DMSO or GW788388. D, Quantification of SOD1 immunoblots in livers of vehicle and 6 h APAP-treated mice injected with DMSO or GW788388. *$p <$ .05 compared with vehicle-treated mice injected with DMSO. #$p <$ .05 compared with 6 h APAP-treated mice injected with DMSO.

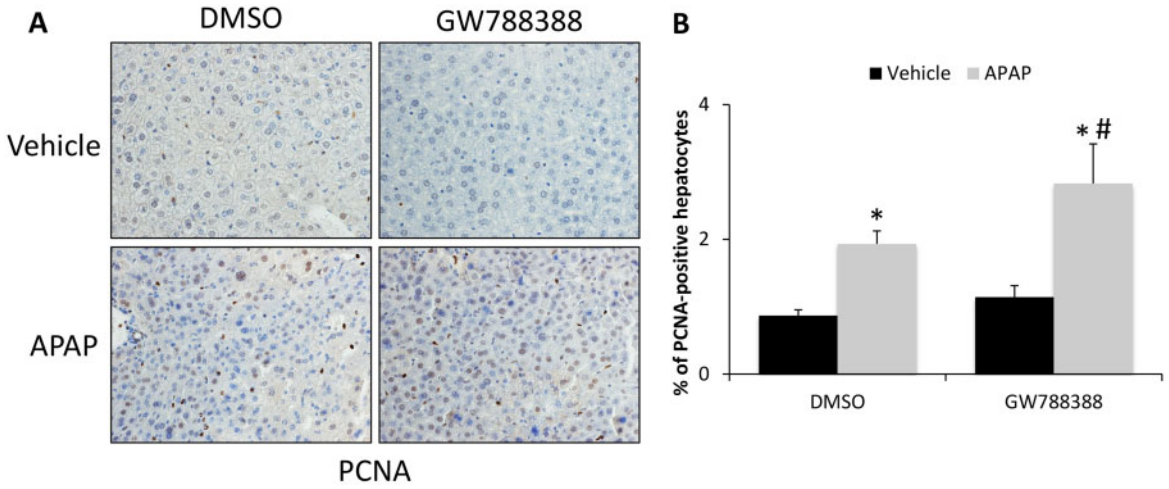

Figure 8. GW788388 treatment increased hepatocyte proliferation in APAP-treated mice. A, PCNA immunohistochemistry in liver sections from vehicle and APAP-treated mice administered DMSO or GW788388. B, Percent of PCNA-positive hepatocytes stained per field in vehicle and APAP-treated mice injected with DMSO or GW788388. *$p <$ .05 compared with vehicle-treated mice injected with DMSO. #$p <$ .05 compared with 6 h APAP-treated mice injected with DMSO.

support that inhibition of TGFβ1 activity or downstream signaling may be beneficial for the management of APAP-induced liver injury.

In the liver TGFβ1 has classically been thought to be involved with hepatic fibrosis with 6- and 10-week administration of APAP at 300 mg/kg found to induce liver fibrosis and the hepatic upregulation of TGFβ1 mRNA in mice (Bai *et al.*, 2017). In the model of azoxymethane-induced ALF with hepatic encephalopathy in mice, the levels of circulating TGFβ1 are increased and using a pan TGFβ or TGFβ1 neutralizing antibody improved survival (McMillin *et al.*, 2014, 2019). In an acute liver injury model involving injection of anti-Fas antibodies, hepatic TGFβ1 mRNA is upregulated and inhibition of TGFβ1 activity reduced hepatic apoptosis and mortality (Grant *et al.*, 2018). Hepatic TGFβ1 mRNA has been shown to be upregulated during CCl_4- and APAP-induced hepatotoxicity with increased mRNA expression being highest after 24 h of treatment (Jeon *et al.*, 1997). Inhibition of TGFβ1 signaling in the liver during APAP-induced ALF has been shown to reduce hepatocyte senescence and improve hepatic function and outcomes in mice (Bird *et al.*, 2018).

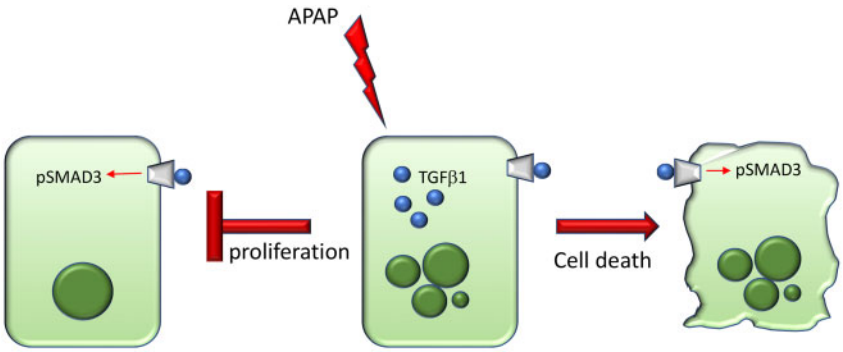

Figure 9. Working schematic of effects of TGFβ1 signaling in APAP-treated mice. During APAP-induced hepatotoxicity, TGFβ1 is increased in injured and dying hepatocytes. Transforming growth factor beta 1 is able to bind the TGFβR1/TGFβR2 heterodimer on hepatocytes resulting in increased phosphorylation of pSMAD3. As a result of induction of TGFβ1 signaling, hepatocyte proliferation is inhibited and cell death is induced. The combination of these deleterious effects exacerbates APAP-induced liver injury.

A recent report demonstrated that activation of latent TGFβ1 by plasma kallikrein occurred during APAP-induced liver injury identifying another level of TGFβ1 signaling regulation in this model (Li *et al.*, 2018). This study demonstrated that TGFβ1 was significantly upregulated during APAP-induced ALF in the liver and that inhibition of TGFβ1 receptor activity by treatment with GW788388 improved outcomes. Taken together, our data support a role of TGFβ1 in APAP-induced necrosis, whereas other studies show a longer upregulation beyond 24 h influencing senescence and regeneration. Collectively, previous studies and this study demonstrate the potential of this pathway as a therapeutic target for management of this disease state outside of the early therapeutic window provided by *N*-acetylcysteine (Smilkstein *et al.*, 1988).

The cellular localization of hepatic TGFβ1 expression is different depending on the disease state of the liver. Independent of disease state, primary hepatocytes and primary hepatic stellate cells have been shown to express and secrete TGFβ1 (Dropmann *et al.*, 2016). During cholestasis due to bile duct ligation in rats and mice, TGFβ1 expression has been shown to be increased and downstream signaling is transduced in cholangiocytes (Luo *et al.*, 2005; Wu *et al.*, 2016). Transforming growth factor beta 1 has been shown to be expressed in primary rat Kupffer cells and exposure to hepatitis B virus particles significantly increased their expression of TGFβ1 (Li *et al.*, 2012). Therefore, it is evident that there may be multiple hepatic sources of TGFβ1 during liver disease and dysfunction. In this study, it was shown that TGFβ1 expression localizes to hepatocytes in the liver during the early stages of APAP-induced injury, though *in situ* hybridization studies find that during later time points macrophages are the primary producer of TGFβ1 (Bird *et al.*, 2018). However, whereas we observed TGFβ1 staining in necrotic areas that was likely a result of infiltrating immune cells, we also observed that hepatocytes in areas away from necrotic tissue stain positive for TGFβ1. This gives support that hepatocytes in APAP-treated mice produce the TGFβ1 ligand even when they are not undergoing necrosis and therefore this allows for these hepatocyte populations to induce signaling in neighboring hepatocytes, possibly contributing to the hepatocyte necrosis observed. This ability of hepatocytes to produce TGFβ1 was validated in this study as primary hepatocytes significantly increased TGFβ1 secretion following APAP administration. One interesting note is that transforming growth factor beta 2 (TGFβ2) has been shown to be expressed in the liver. Transforming growth factor beta 2 mRNA and protein have been shown to be upregulated during bile duct ligation in rats (Zepeda-Morales *et al.*, 2016). In addition both TGFβ1 and TGFβ2 have been shown to be significantly upregulated 24 h following CCl_4 injection (Dropmann *et al.*, 2016). A greater characterization of the specific role of each TGFβ ligand in the context of APAP-induced liver injury could provide additional insight into this signaling pathway during this disease state.

One of the core characteristics of APAP-induced ALF is the presence of centrilobular hepatocyte necrosis. This observation occurs at both lower (300 mg/kg) and higher (600 mg/kg) concentrations of APAP in mice (Bhushan *et al.*, 2014). The process of necrosis has been determined to be a consequence of high concentrations of APAP being metabolized to the toxic metabolite NAPQI, which results in the depletion of GSH, the formation of protein adducts, increased oxidative stress and decreased mitochondrial respiration (Davis *et al.*, 1974; Meyers *et al.*, 1988; Yan *et al.*, 2010). During this state of oxidative stress there is activation of the MAP kinase JNK, a key driver of hepatocyte necrosis. Administration of the JNK inhibitor SP600125 to mice injected with 800 mg/kg APAP was found to significantly reduce hepatic necrosis without influencing GSH levels (Gunawan *et al.*, 2006). This improvement in the degree of necrosis without influencing GSH was similar to what we observed in our APAP-treated mice administered GW788388. In contrast, given that we observed an attenuation of APAP-induced suppression of Cyp2E1 expression by GW788388 treatment without the concomitant rescue of GSH depletion, we would suggest that the changes in Cyp2E1 in our treatment groups are likely a reflection of reduced hepatocyte necrosis observed in GW788388-treated mice.

Although the activation of JNK signaling has been shown during APAP-induced liver injury, there are other pathways that can influence JNK signaling such as IL-1, TNF, and TGFβ1 (Jiang *et al.*, 2017; Tada *et al.*, 2001). We find that the pJNK to JNK ratio is increased during APAP-induced liver injury, as others have shown, and pretreatment with GW788388 in APAP-treated mice significantly reduced pJNK expression compared with DMSO-treated mice administered APAP. It is possible that total hepatic JNK levels may change during APAP-induced necrosis or due to treatments during this disease state. That being said, significant changes in total JNK due to APAP or GW788388 administration were not observed in this study. As TGFβ1 has been shown to induce pJNK signaling, it is likely that inhibition of TGFβR1 via GW788388 inhibited this signaling pathway leading to the reduction of hepatic necrosis observed in GW788388-treated mice.

Hepatic inflammation is associated with many forms of liver injury including ischemia-reperfusion injury, viral hepatitis, primary biliary cirrhosis, primary sclerosing cholangitis, and other liver disorders. During APAP-induced liver injury, inflammation is induced but may be considered beneficial due to macrophages digesting cellular debris of necrotic tissue to help stimulate regeneration. In patients with APAP-induced ALF, there is a significant increase in hepatic TGFβ1 protein, increased proliferation of resident and infiltrating macrophages and increased pro-inflammatory cytokine expression (Antoniades *et al.*, 2012). In this study, APAP administration generated an increase in both TNFα and IL-1β, which were able to be significantly reduced in mice were pretreated with GW788388. Serum and hepatic expression of TNFα has been demonstrated to increase in APAP-treated mice (Yan *et al.*, 2016). Increases in pro-IL-1β have been shown during APAP-induced liver injury and mice with genetic knockout of toll-like receptor 9 have reduced pro-IL-1β expression, reduced serum ALT levels and improved survival compared with wild type mice (Imaeda *et al.*, 2009). However, mice with genetic knockout of the receptor for IL-1 administered 300 mg/kg APAP have no differences in plasma ALT levels or hepatic necrosis when compared with wild type mice administered APAP (Williams *et al.*, 2010). Transforming growth factor beta 1 signaling can induce pro-inflammatory signaling as during CCl_4-induced liver injury in mice, SMAD3 overexpression led to increased circulating IL-1β and IL-6 levels compared with wild type mice (Niu *et al.*, 2016). That being said, it is still not clear whether modulating the immune response leads to an improvement in outcomes during APAP-induced liver injury. Based on the current understanding of the role of inflammation during APAP-induced liver injury, it is likely that the effects regarding necrosis and regeneration by GW788388 treatment are more important in improving outcomes than modulating the inflammatory response. More studies are necessary to characterize the interaction between inflammation, TGFβ1 signaling, and liver injury in this model.

Hepatotoxicity from APAP is associated with a great degree of oxidative stress. Rapidly following APAP administration in mice there is a dose-dependent increase in reactive oxygen species and reactive nitrogen species prior to overt histological changes (Shuhendler *et al.*, 2014). In addition to this, NAPQI has the ability to form protein adducts in mitochondria, impairing cellular respiration resulting in increased reactive oxygen species production (Neal *et al.*, 2015; Qiu *et al.*, 1998). In this study, we identified that the antioxidant SOD1 was significantly decreased in APAP-treated mice and that GW788388 treatment was able to increase SOD1 expression. Although the mechanism was not identified, it is possible that antagonism of SMAD signaling with GW788388 increased Nrf2 signaling as there is an antagonistic relationship between these 2 signaling pathways as established in multiple animal models (Chen *et al.*, 2017; Prestigiacomo and Suter-Dick, 2018; Wang *et al.*, 2016). In addition, inhibition of Nrf2 with siRNA in mice demonstrated that levels of SOD1 protein were decreased (Xue *et al.*, 2016). Interestingly, GW788388 treatment alone reduced GSH levels in the livers of vehicle-treated mice, suggesting a possible interaction with Nrf2 and GSH metabolism, though this would be contradictory to the protective effect of GW788388 treatment observed in all other measures of liver toxicity studied. That being said, more mechanistic studies are needed to fully classify the role of TGFβ1 signaling in oxidative stress associated with APAP-induced liver injury.

Hepatic regeneration is a key component of the resolution of APAP-induced ALF. In sublethal doses of APAP in rodents, serum ALT concentrations and necrosis generally peak around 12 h post-injection and return to normal levels in approximately 72 h post-injury in mice administered 300 mg/kg APAP (Bhushan *et al.*, 2014, 2017). Transforming growth factor beta 1 has been shown to directly inhibit DNA synthesis in primary hepatocytes and the application of the thrombospondin-1 antagonist LSKL, which would inhibit TGFβ1 activation, facilitated liver regeneration at up to 48 h post 70% partial hepatectomy in mice (Kuroki *et al.*, 2015; McMahon *et al.*, 1986). In addition, p21 expression as a marker of senescence is increased in APAP-induced liver injury and inhibition of TGFβR1 reduced p21 expression and increased 5-bromo-2′-deoxyuridine staining in hepatocytes (Bird *et al.*, 2018). These previous studies support that TGFβ1 could promote APAP-induced liver injury by inhibiting regeneration of the liver. This was supported by data from this study where PCNA staining was increased in APAP-treated mice. In addition to this, inhibition of TGFβ1 signaling with GW788388 treatment led to an even greater increase in PCNA-positive hepatocytes. Together, these data indicate that TGFβ1 can inhibit hepatocyte proliferation and therefore could influence the regenerative phase of APAP-induced liver injury.

In conclusion, TGFβ1 was upregulated during APAP-induced hepatic injury and induced downstream signaling in hepatocytes neighboring necrotic areas. Inhibition of TGFβ1 signaling with GW788388 improved multiple aspects of APAP pathology including necrosis, inflammation, oxidative stress, and regeneration, which ultimately resulted in reduced liver injury. Therefore, targeting the TGFβ1 ligand or its downstream receptor-mediated signaling may be an effective therapeutic target to improve the management of APAP-induced ALF.

DECLARATION OF CONFLICTING INTERESTS

The author/authors declared no potential conflicts of interest with respect to the research, authorship, and/or publication of this article.

ACKNOWLEDGMENTS

This work was completed with support from the Veterans Health Administration and with resources and the use of facilities at the Central Texas Veterans Health Care System, Temple, Texas. The contents do not represent the views of the U.S. Department of Veterans Affairs or the United States Government.

FUNDING

This study was funded by NIH R01 awards (DK082435 and DK112803) and a VA Merit award (BX002638 to S.D.) from the U.S. Department of Veterans Affairs Biomedical Laboratory Research and Development Service. This study was also funded by a VA Career Development award (BX003486 to M.M) from the U.S. Department of Veterans Affairs Biomedical Laboratory Research and Development Service.

REFERENCES

Abdollah, S., Macias-Silva, M., Tsukazaki, T., Hayashi, H., Attisano, L., and Wrana, J. L. (1997). TbetaRI phosphorylation of Smad2 on Ser465 and Ser467 is required for Smad2-Smad4 complex formation and signaling. *J. Biol. Chem.* **272**, 27678–27685.

Antoniades, C. G., Quaglia, A., Taams, L. S., Mitry, R. R., Hussain, M., Abeles, R., Possamai, L. A., Bruce, M., McPhail, M., Starling, C., *et al.* (2012). Source and characterization of hepatic macrophages in acetaminophen-induced acute liver failure in humans. *Hepatology* **56**, 735–746.

Bai, Q., Yan, H., Sheng, Y., Jin, Y., Shi, L., Ji, L., and Wang, Z. (2017). Long-term acetaminophen treatment induced liver fibrosis in mice and the involvement of Egr-1. *Toxicology* **382**, 47–58.

Bajt, M. L., Cover, C., Lemasters, J. J., and Jaeschke, H. (2006). Nuclear translocation of endonuclease G and apoptosis-inducing factor during acetaminophen-induced liver cell injury. *Toxicol. Sci.* **94**, 217–225.

Bajt, M. L., Farhood, A., Lemasters, J. J., and Jaeschke, H. (2007). Mitochondrial Bax translocation accelerates DNA fragmentation and cell necrosis in a murine model of acetaminophen hepatotoxicity. *J. Pharmacol. Exp. Ther.* **324**, 8–14.

Bernal, W., Auzinger, G., Dhawan, A., and Wendon, J. (2010). Acute liver failure. *Lancet* **376**, 190–201.

Bernal, W., Lee, W. M., Wendon, J., Larsen, F. S., and Williams, R. (2015). Acute liver failure: A curable disease by 2024? *J. Hepatol.* **62**, S112–120.

Bhushan, B., Chavan, H., Borude, P., Xie, Y., Du, K., McGill, M. R., Lebofsky, M., Jaeschke, H., Krishnamurthy, P., and Apte, U. (2017). Dual role of epidermal growth factor receptor in liver injury and regeneration after acetaminophen overdose in mice. *Toxicol. Sci.* **155**, 363–378.

Bhushan, B., Walesky, C., Manley, M., Gallagher, T., Borude, P., Edwards, G., Monga, S. P., and Apte, U. (2014). Pro-regenerative signaling after acetaminophen-induced acute liver injury in mice identified using a novel incremental dose model. *Am. J. Pathol.* **184**, 3013–3025.

Bird, T. G., Muller, M., Boulter, L., Vincent, D. F., Ridgway, R. A., Lopez-Guadamillas, E., Lu, W. Y., Jamieson, T., Govaere, O., Campbell, A. D., *et al.* (2018). TGFbeta inhibition restores a regenerative response in acute liver injury by suppressing paracrine senescence. *Sci. Transl. Med.* **10**, 454.

Blazka, M. E., Wilmer, J. L., Holladay, S. D., Wilson, R. E., and Luster, M. I. (1995). Role of proinflammatory cytokines in acetaminophen hepatotoxicity. *Toxicol. Appl. Pharmacol.* **133**, 43–52.

Boyd, E. M., and Bereczky, G. M. (1966). Liver necrosis from paracetamol. *Br. J. Pharmacol. Chemother.* **26**, 606–614.

Chen, Q., Zhang, H., Cao, Y., Li, Y., Sun, S., Zhang, J., and Zhang, G. (2017). Schisandrin B attenuates CCl4-induced liver fibrosis in rats by regulation of Nrf2-ARE and TGF-beta/Smad signaling pathways. *Drug Des. Dev. Ther.* **11**, 2179–2191.

Dahlin, D. C., Miwa, G. T., Lu, A. Y., and Nelson, S. D. (1984). N-acetyl-p-benzoquinone imine: A cytochrome p-450-mediated oxidation product of acetaminophen. *Proc. Natl. Acad. Sci. U.S.A.* **81**, 1327–1331.

Davis, D. C., Potter, W. Z., Jollow, D. J., and Mitchell, J. R. (1974). Species differences in hepatic glutathione depletion, covalent binding and hepatic necrosis after acetaminophen. *Life Sci.* **14**, 2099–2109.

Dropmann, A., Dediulia, T., Breitkopf-Heinlein, K., Korhonen, H., Janicot, M., Weber, S. N., Thomas, M., Piiper, A., Bertran, E., Fabregat, I., *et al.* (2016). TGF-beta1 and TGF-beta2 abundance in liver diseases of mice and men. *Oncotarget* **7**, 19499–19518.

Du, K., Ramachandran, A., and Jaeschke, H. (2016). Oxidative stress during acetaminophen hepatotoxicity: Sources, pathophysiological role and therapeutic potential. *Redox Biol.* **10**, 148–156.

Du, K., Williams, C. D., McGill, M. R., and Jaeschke, H. (2014). Lower susceptibility of female mice to acetaminophen hepatotoxicity: Role of mitochondrial glutathione, oxidant stress and c-jun N-terminal kinase. *Toxicol. Appl. Pharmacol.* **281**, 58–66.

Grant, S., McMillin, M., Frampton, G., Petrescu, A. D., Williams, E., Jaeger, V., Kain, J., and DeMorrow, S. (2018). Direct comparison of the thioacetamide and azoxymethane models of type a hepatic encephalopathy in mice. *Gene Expr.* **18**, 171–185.

Gunawan, B. K., Liu, Z. X., Han, D., Hanawa, N., Gaarde, W. A., and Kaplowitz, N. (2006). c-Jun N-terminal kinase plays a major role in murine acetaminophen hepatotoxicity. *Gastroenterology* **131**, 165–178.

Imaeda, A. B., Watanabe, A., Sohail, M. A., Mahmood, S., Mohamadnejad, M., Sutterwala, F. S., Flavell, R. A., and Mehal, W. Z. (2009). Acetaminophen-induced hepatotoxicity in mice is dependent on Tlr9 and the Nalp3 inflammasome. *J. Clin. Invest.* **119**, 305–314.

Jablonska, E., Markart, P., Zakrzewicz, D., Preissner, K. T., and Wygrecka, M. (2010). Transforming growth factor-beta1 induces expression of human coagulation factor XII via Smad3 and JNK signaling pathways in human lung fibroblasts. *J. Biol. Chem.* **285**, 11638–11651.

Jeon, Y. J., Han, S. H., Yang, K. H., and Kaminski, N. E. (1997). Induction of liver-associated transforming growth factor beta 1 (TGF-beta 1) mRNA expression by carbon tetrachloride leads to the inhibition of T helper 2 cell-associated lymphokines. *Toxicol. Appl. Pharmacol.* **144**, 27–35.

Jiang, X., Huang, B., Yang, H., Li, G., Zhang, C., Yang, G., Lin, F., and Lin, G. (2017). TGF-beta1 is involved in vitamin D-induced chondrogenic differentiation of bone marrow-derived mesenchymal stem cells by regulating the ERK/JNK pathway. *Cell. Physiol. Biochem.* **42**, 2230–2241.

Kon, K., Kim, J. S., Jaeschke, H., and Lemasters, J. J. (2004). Mitochondrial permeability transition in acetaminophen-induced necrosis and apoptosis of cultured mouse hepatocytes. *Hepatology* **40**, 1170–1179.

Kuroki, H., Hayashi, H., Nakagawa, S., Sakamoto, K., Higashi, T., Nitta, H., Hashimoto, D., Chikamoto, A., Beppu, T., and Baba, H. (2015). Effect of LSKL peptide on thrombospondin 1-mediated transforming growth factor beta signal activation and liver regeneration after hepatectomy in an experimental model. *Br. J. Surg.* **102**, 813–825.

Li, H., Zheng, H. W., Chen, H., Xing, Z. Z., You, H., Cong, M., and Jia, J. D. (2012). Hepatitis B virus particles preferably induce kupffer cells to produce TGF-beta1 over pro-inflammatory cytokines. *Dig. Liver Dis.* **44**, 328–333.

Li, M., Qin, X. Y., Furutani, Y., Inoue, I., Sekihara, S., Kagechika, H., and Kojima, S. (2018). Prevention of acute liver injury by suppressing plasma kallikrein-dependent activation of latent TGF-beta. *Biochem. Biophys. Res. Commun.* **504**, 857–864.

Luo, B., Tang, L., Wang, Z., Zhang, J., Ling, Y., Feng, W., Sun, J. Z., Stockard, C. R., Frost, A. R., Chen, Y. F., *et al.* (2005). Cholangiocyte endothelin 1 and transforming growth factor beta1 production in rat experimental hepatopulmonary syndrome. *Gastroenterology* **129**, 682–695.

McCord, J. M., and Fridovich, I. (1969). Superoxide dismutase. An enzymic function for erythrocuprein (hemocuprein). *J. Biol. Chem.* **244**, 6049–6055.

McMahon, J. B., Richards, W. L., del Campo, A. A., Song, M. K., and Thorgeirsson, S. S. (1986). Differential effects of transforming growth factor-beta on proliferation of normal and malignant rat liver epithelial cells in culture. *Cancer Res.* **46**, 4665–4671.

McMillin, M., Galindo, C., Pae, H. Y., Frampton, G., Di Patre, P. L., Quinn, M., Whittington, E., and DeMorrow, S. (2014). Gli1 activation and protection against hepatic encephalopathy is suppressed by circulating transforming growth factor beta1 in mice. *J. Hepatol.* **61**, 1260–1266.

McMillin, M., Grant, S., Frampton, G., Petrescu, A. D., Williams, E., Jefferson, B., Thomas, A., Brahmaroutu, A., and DeMorrow, S. (2019). Elevated circulating TGFbeta1 during acute liver failure activates TGFbetar2 on cortical neurons and exacerbates neuroinflammation and hepatic encephalopathy in mice. *J. Neuroinflamm.* **16**, 69.

Meyers, L. L., Beierschmitt, W. P., Khairallah, E. A., and Cohen, S. D. (1988). Acetaminophen-induced inhibition of hepatic mitochondrial respiration in mice. *Toxicol. Appl. Pharmacol.* **93**, 378–387.

Miwa, Y., Harrison, P. M., Farzaneh, F., Langley, P. G., Williams, R., and Hughes, R. D. (1997). Plasma levels and hepatic mRNA expression of transforming growth factor-beta1 in patients with fulminant hepatic failure. *J. Hepatol.* **27**, 780–788.

Nakagawa, H., Maeda, S., Hikiba, Y., Ohmae, T., Shibata, W., Yanai, A., Sakamoto, K., Ogura, K., Noguchi, T., Karin, M., *et al.* (2008). Deletion of apoptosis signal-regulating kinase 1 attenuates acetaminophen-induced liver injury by inhibiting c-jun N-terminal kinase activation. *Gastroenterology* **135**, 1311–1321.

Neal, A., Rountree, A. M., Philips, C. W., Kavanagh, T. J., Williams, D. P., Newham, P., Khalil, G., Cook, D. L., and Sweet, I. R. (2015). Quantification of low-level drug effects using real-time, *in vitro* measurement of oxygen consumption rate. *Toxicol. Sci.* **148**, 594–602.

Niu, L., Cui, X., Qi, Y., Xie, D., Wu, Q., Chen, X., Ge, J., and Liu, Z. (2016). Involvement of TGF-beta1/Smad3 signaling in carbon tetrachloride-induced acute liver injury in mice. *PLoS One* **11**, e0156090.

Prestigiacomo, V., and Suter-Dick, L. (2018). Nrf2 protects stellate cells from Smad-dependent cell activation. *PLoS One* **13**, e0201044.

Qiu, Y., Benet, L. Z., and Burlingame, A. L. (1998). Identification of the hepatic protein targets of reactive metabolites of acetaminophen *in vivo* in mice using two-dimensional gel electrophoresis and mass spectrometry. *J. Biol. Chem.* **273**, 17940–17953.

Shuhendler, A. J., Pu, K., Cui, L., Uetrecht, J. P., and Rao, J. (2014). Real-time imaging of oxidative and nitrosative stress in the liver of live animals for drug-toxicity testing. *Nat. Biotechnol.* **32**, 373–380.

Smilkstein, M. J., Knapp, G. L., Kulig, K. W., and Rumack, B. H. (1988). Efficacy of oral *N*-acetylcysteine in the treatment of acetaminophen overdose. Analysis of the national multicenter study (1976 to 1985). *N. Engl. J. Med.* **319**, 1557–1562.

Tada, K., Okazaki, T., Sakon, S., Kobarai, T., Kurosawa, K., Yamaoka, S., Hashimoto, H., Mak, T. W., Yagita, H., Okumura, K., *et al.* (2001). Critical roles of TRAF2 and TRAF5 in tumor necrosis factor-induced NF-kappa B activation and protection from cell death. *J. Biol. Chem.* **276**, 36530–36534.

Wang, Z., Zhang, H., Sun, X., and Ren, L. (2016). The protective role of vitamin D3 in a murine model of asthma via the suppression of TGF-beta/Smad signaling and activation of the Nrf2/HO-1 pathway. *Mol. Med. Rep.* **14**, 2389–2396.

Williams, C. D., Farhood, A., and Jaeschke, H. (2010). Role of caspase-1 and interleukin-1beta in acetaminophen-induced hepatic inflammation and liver injury. *Toxicol. Appl. Pharmacol.* **247**, 169–178.

Wu, N., Meng, F., Invernizzi, P., Bernuzzi, F., Venter, J., Standeford, H., Onori, P., Marzioni, M., Alvaro, D., Franchitto, A., *et al.* (2016). The secretin/secretin receptor axis modulates liver fibrosis through changes in transforming growth factor-beta1 biliary secretion in mice. *Hepatology* **64**, 865–879.

Xie, Y., McGill, M. R., Dorko, K., Kumer, S. C., Schmitt, T. M., Forster, J., and Jaeschke, H. (2014). Mechanisms of acetaminophen-induced cell death in primary human hepatocytes. *Toxicol. Appl. Pharmacol.* **279**, 266–274.

Xue, F., Huang, J. W., Ding, P. Y., Zang, H. G., Kou, Z. J., Li, T., Fan, J., Peng, Z. W., and Yan, W. J. (2016). Nrf2/antioxidant defense pathway is involved in the neuroprotective effects of Sirt1 against focal cerebral ischemia in rats after hyperbaric oxygen preconditioning. *Behav. Brain Res.* **309**, 1–8.

Yan, H. M., Ramachandran, A., Bajt, M. L., Lemasters, J. J., and Jaeschke, H. (2010). The oxygen tension modulates acetaminophen-induced mitochondrial oxidant stress and cell injury in cultured hepatocytes. *Toxicol. Sci.* **117**, 515–523.

Yan, T., Wang, H., Zhao, M., Yagai, T., Chai, Y., Krausz, K. W., Xie, C., Cheng, X., Zhang, J., Che, Y., *et al.* (2016). Glycyrrhizin protects against acetaminophen-induced acute liver injury via alleviating tumor necrosis factor alpha-mediated apoptosis. *Drug Metab. Dispos.* **44**, 720–731.

Yu, X., Guo, R., Ming, D., Deng, Y., Su, M., Lin, C., Li, J., Lin, Z., and Su, Z. (2015). The transforming growth factor beta1/interleukin-31 pathway is upregulated in patients with hepatitis B virus-related acute-on-chronic liver failure and is associated with disease severity and survival. *Clin. Vaccine Immunol.* **22**, 484–492.

Zepeda-Morales, A. S., Del Toro-Arreola, S., Garcia-Benavides, L., Bastidas-Ramirez, B. E., Fafutis-Morris, M., Pereira-Suarez, A. L., and Bueno-Topete, M. R. (2016). Liver fibrosis in bile duct-ligated rats correlates with increased hepatic IL-17 and TGF-beta2 expression. *Ann. Hepatol.* **15**, 418–426.

Zhang, Y., Feng, X., We, R., and Derynck, R. (1996). Receptor-associated mad homologues synergize as effectors of the TGF-beta response. *Nature* **383**, 168–172.